

# Effect of H on the crystalline and magnetic structures of the $\text{YCo}_3\text{-H(D)}$ system. I. $\text{YCo}_3$ from neutron powder diffraction and first-principles calculations

Xiang-Yuan Cui, Jian Liu, Peter A. Georgiev, Ian Morrison,\* and D. Keith Ross

*Institute for Materials Research, Joule Physics Laboratory, University of Salford, Salford, M5 4WT, United Kingdom*

Mark A. Roberts

*SRS, Daresbury Laboratory, Warrington, Cheshire, WA4 4AD, United Kingdom*

Ken A. Andersen and Mark Telling

*ISIS, Rutherford Appleton Laboratory, Chilton, Didcot, Oxfordshire OX11 0QX, United Kingdom*

Dave Fort

*School of Metallurgy and Materials, University of Birmingham, Edgbaston, Birmingham, B15 2TT, United Kingdom*

(Received 25 May 2007; published 30 November 2007)

This paper reports investigations into the influence of hydrogen on the magnetic properties of the  $\text{YCo}_3\text{-H}$  system. We report results on the magnetic structure and magnetic transitions of  $\text{YCo}_3$  using a combination of neutron powder diffraction measurements and first-principles full potential augmented plane wave + local orbital calculations under the generalized gradient approximation. The ferromagnetic and ferrimagnetic structures are examined on an equal footing. However, we identify that, no matter which structure is used as the starting point, the neutron diffraction data always refines down to the ferrimagnetic structure with the  $\text{Co}_2$  atoms having antiparallel spins. In the *ab initio* calculations, the inclusion of spin-orbit coupling is found to be important in the prediction of the correct magnetic ground state. Here, the results suggest that, for zero external field and sufficiently low temperatures, the spin arrangement of  $\text{YCo}_3$  is ferrimagnetic rather than ferromagnetic as previously believed. The fixed spin moment calculation technique has been employed to understand the two successive field-induced magnetic transitions observed in previous magnetization measurements under increasing ultrahigh magnetic fields. We find that the magnetic transitions start from the ferrimagnetic phase ( $0.61\mu_B/\text{Co}$ ) and terminate with the ferromagnetic phase ( $1.16\mu_B/\text{Co}$ ), while the spin on the  $\text{Co}_2$  atoms progressively changes from antiparallel ferrimagnetic to paramagnetic and then to ferromagnetic. Our neutron diffraction measurements, *ab initio* calculations, and the high field magnetization measurements are thus entirely self-consistent.

DOI: [10.1103/PhysRevB.76.184443](https://doi.org/10.1103/PhysRevB.76.184443)

PACS number(s): 75.50.Gg, 75.10.-b, 71.20.-b, 61.12.Ld

## I. INTRODUCTION

The intermetallic compound  $\text{YCo}_3$  has recently attracted renewed interest for two main reasons. Firstly, it demonstrates dramatic changes in its magnetic properties upon hydrogenation<sup>1-3</sup> and secondly, it undergoes metamagnetic transitions in high magnetic fields.<sup>2</sup> Experiments show that  $\text{YCo}_3\text{H}_x$ , for  $x=0$ , is either ferromagnetic or ferrimagnetic while, in the  $\beta_1$  phase (where  $1.0 < x < 1.3$ ), it is paramagnetic (or possibly antiferromagnetic with a Néel temperature of 273 K), in the  $\beta_2$  phase (with  $1.5 < x < 2.0$ ), it is ferromagnetic, having a Curie temperature of 237 K (but note that recent studies alternatively suggest that ferromagnetism and paramagnetism may coexist in this phase<sup>4</sup>), and finally, in the  $\gamma$  phase (having  $3.5 < x < 4.0$ ), it is antiferromagnetic with a Néel temperature of 200 K. This novel behavior has some parallels with the changes in the electrical conductivity and optical properties of Y/H thin film systems driven by varying hydrogen content.<sup>5</sup> In view of the spectacular changes in the magnetic properties that can, in principle, be controlled electrochemically or by changing hydrogen pressure, the  $\text{YCo}_3/\text{H}$  system may find important technological applications.

In Part I of this study, we are concerned with understanding the magnetic properties of the basic compound  $\text{YCo}_3$ . As

one can see below, even for the parent crystal  $\text{YCo}_3$ , there are conflicting views as to whether the magnetic ground state is ferromagnetic or ferrimagnetic. In Part II,<sup>6</sup> we report on investigations into the crystal and magnetic structures of this system as a function of increasing hydrogen content by means of synchrotron x-ray and neutron diffraction distinguishing between the so-called  $\beta_1$  and  $\beta_2$  phases with the objective of understanding what drives the dramatic changes in magnetization that are observed.

Regarding the magnetic ground state of  $\text{YCo}_3$ , a survey of the previous literature reveals this to be a controversial issue, from both the experimental and theoretical points of view. There are two well-known but contradictory experimental studies. Lemaire<sup>7</sup> first observed the compound to have a ferrimagnetic character by studying the behavior of the magnetization as a function of temperature using polycrystalline specimens. When measured as a function of temperature, he observed that the magnetization passes through a maximum at approximately 170 K in a field of 2 T. This experiment has been recently repeated in our group at 6 T with similar results.<sup>3</sup> On the other hand, based on polarized neutron diffraction measurements on a single crystal sample, Kren *et al.* concluded that  $\text{YCo}_3$  was ferromagnetic.<sup>8</sup> Here the measured magnetic moments for the Co atoms were  $\text{Co}_1: 0.55\mu_B$ ,

Co<sub>2</sub>:  $0.8\mu_B$ , Co<sub>3</sub>:  $0.4\mu_B$ . Note in their data refinement, the atomic position parameters in YCo<sub>3</sub> are assumed to be the same as in HoCo<sub>3</sub>. Furthermore, no effort was apparently made during the fitting process to search for a possible ferrimagnetic solution.

A number of theoretical studies have also been performed on the electronic structure and magnetic spin distributions in YCo<sub>3</sub>.<sup>9–12</sup> However, again, only the ferromagnetic phase has been investigated and significant discrepancies exist between these previous theoretical calculations. By assuming a simple FCC Cu<sub>3</sub>Au structure, rather than the real PuNi<sub>3</sub> structure, Moruzzi *et al.*<sup>13</sup> first obtained an average magnetic moment (MM)  $0.83\mu_B/\text{Co}$  and found a magnetic instability induced by volume change. Inoue and Shimizu<sup>9</sup> obtained an average value of  $0.83\mu_B/\text{Co}$  using the recursion method. Coehoorn<sup>10</sup> obtained a value of  $1.05\mu_B/\text{Co}$ , using the augmented spherical wave method within the local-spin-density-approximation (LSDA) framework. However, Yamaguchi and Asano,<sup>11</sup> employing the linear muffin-tin orbital method at the atomic sphere approximation within the LSDA scheme, obtained  $0.64\mu_B/\text{Co}$ , this value being the closest to the experimental value for the bulk magnetization. Note that the results given in Refs. 10 and 11 were obtained without performing any structural relaxation of either lattice constants or atomic coordinates.

Thus, despite the number of publications on this subject, no general consensus has yet been reached. To resolve these discrepancies, we have examined the ground state magnetization and the magnetic structure of YCo<sub>3</sub> in a balanced way. Both the ferromagnetic and ferrimagnetic phases have been used as starting points in the refinement of the neutron diffraction data and in the first-principles calculations. Often the magnetic structure of a system obtained by refinement of neutron diffraction data is obtained within predictable errors, particularly where only polycrystalline samples are available. Hence theoretical total energy calculations can be important in supporting or refuting the magnetic structure suggested by experiments as well as revealing the mechanism that drives a specific behavior. This is particularly true for YCo<sub>3</sub> as will become apparent below.

Further motivation for this work is aimed to understand the interesting magnetic transitions undergone by YCo<sub>3</sub> in an externally applied field as observed by Goto *et al.*<sup>12</sup> In an increasing magnetic field measured up to 110 T, two successive magnetic transitions are observed, without hysteresis. The magnetization is observed to increase from 0.72 to  $0.88\mu_B/\text{Co}$  at 60 T and from 0.88 to  $1.23\mu_B/\text{Co}$  at 82 T. A rigid band model, based on the density of states (DOS) of the ferromagnetic phase, could only explain one transition.<sup>12</sup> As the authors noted, theoretical studies of the electronic structure and of the magnetic properties in ultrahigh magnetic fields are needed to clarify the mechanism involved here.

Theoretically, the fixed spin moment (FSM) procedure, first introduced by Schwartz and Mohn,<sup>14</sup> can be regarded as the equivalent of performing calculations of the equilibrium structure in a series of applied magnetic fields. The FSM procedure is a powerful and sensitive way of finding and tracing magnetic phases and of determining their stability and existence limits. The method has been widely employed in calculations of magnetic structure.<sup>15</sup> In this paper, we re-

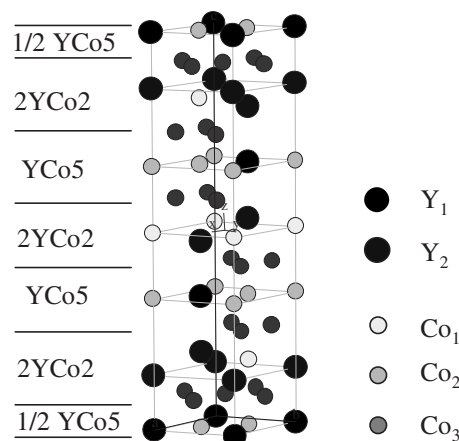


FIG. 1. Crystal structure of the YCo<sub>3</sub>. It can be conveniently described in terms of the alternate stacking of YCo<sub>5</sub> cells of the CaCu<sub>5</sub> type and YCo<sub>2</sub> cells of the MgCu<sub>2</sub> type structure.

port FSM results for both the ferromagnetic and the ferrimagnetic phases of YCo<sub>3</sub>.

The crystal structure of YCo<sub>3</sub> can be summarized as follows: it has the rhombohedral *R-3m* space group, usually presented in hexagonal coordinates, and conveniently described in terms of alternate stacking of YCo<sub>5</sub> cells of the CaCu<sub>5</sub> structure type and YCo<sub>2</sub> cells of the MgCu<sub>2</sub> structure type in the ratio 1:2 (see Fig. 1). The structure is isomorphous with PuNi<sub>3</sub>, having two different sites for the Y atoms (Y<sub>1</sub> at *3a* and Y<sub>2</sub> at *6c*) and three for Co atoms (Co<sub>1</sub> at *3b*, Co<sub>2</sub> at *6c*, and Co<sub>3</sub> at *18h*).

The rest of Part I of this paper is organized as follows. Experimental details and results are described in Sec. II. Section III contains details of the calculations, the results, and comparisons with the experimental findings. Further discussion is presented in Sec. IV and finally, the main conclusions are summarized in Sec. V.

## II. EXPERIMENTAL DETAILS AND RESULTS

The polycrystalline compound YCo<sub>3</sub> was prepared by arc melting Y (+99.9% purity) and Co (+99.9% purity) metal pieces in an argon atmosphere, followed by annealing at 1050 °C in an argon atmosphere for seven days and then crushing into powders of dimension smaller than 45 μm. Synchrotron x-ray-diffraction measurements were made at room temperature at Station 9.1, at the SRS, U.K., using a capillary sample container. The analysis of the synchrotron x-ray data showed that the sample powder contained extraneous phases of YCo<sub>5</sub>, Y<sub>2</sub>Co<sub>7</sub>, and YCo<sub>2</sub> amounting to about 5% by mass. The experimental diffraction pattern was refined using GSAS.<sup>16</sup> The resulting lattice parameters are given in Table I.

The neutron powder diffraction (NPD) experiments were carried out on the OSIRIS diffractometer, ISIS, U.K., with a cryostat for the low temperature measurements. The NPD patterns, taken at temperatures above the Curie temperatures, were used to refine the crystal structure. Diffraction patterns were also recorded at temperatures below the Curie point in

TABLE I. Calculated crystallographic data for YCo<sub>3</sub> from *ab initio* calculations, compared with synchrotron x-ray-diffraction (SXR) results.

	Experimental SXR	Calculated
$a$ (Å)	5.016	5.020
$c$ (Å)	24.373	24.250
Y <sub>1</sub> ( $3a$ )	0,0,0	0,0,0
Y <sub>2</sub> ( $6c$ )	0,0,0.1411	0,0,0.1399
Co <sub>1</sub> ( $3b$ )	0,0,0.5	0,0,0.5
Co <sub>2</sub> ( $6c$ )	0,0,0.3337	0,0,0.3346
Co <sub>3</sub> ( $18h, x, -x, z$ )	0.5006, 0.4994, 0.0815	0.5034, 0.4966, 0.0803

zero field to avoid the introduction of preferred orientation. To determine the crystalline and magnetic structures, the NPD patterns were refined using GSAS.<sup>16</sup> The resultant data are recorded in Table II. The experimental procedures are described in more detail in Part II.

With reference to previous measurements of the temperature and field dependence of the magnetization, it should be noted that a peak is seen in Lemaire's measurement in 2 T at around 130 K (Ref. 7) and in our measurement on YCo<sub>3</sub> powder in 6 T at around 150 K (see Fig. 4 in Ref. 3) but no such peak was observed in measurements on a YCo<sub>3</sub> single crystal at 1 T by Bartashevich *et al.*<sup>17</sup> or in our previous measurements on YCo<sub>3</sub> powder at 0.1 T.<sup>3</sup> It would therefore appear that this maximum only occurs at higher fields. There are two possible explanations for this behavior. The first is that YCo<sub>3</sub> is ferrimagnetic in nature. At low fields, as the temperature is increased, the ordering of the parallel and antiparallel magnetic moments disappears at the same rate and so the ferrimagnetic characteristics are disguised, resulting in the behavior being indistinguishable from a ferromagnetic response. At high fields, however, the applied field reduces the energy of the ferromagnetic state relative to the ferrimagnetic state and so the antiparallel magnetic moment becomes disordered at a lower temperature than the ferromagnetism of the Co<sub>1</sub> and Co<sub>3</sub> atoms. The second possibility is that YCo<sub>3</sub>

is always ferromagnetic in nature, and the peak at 130 K is caused by the effect of the magnetic anisotropy in a high field. The anisotropy field decreases with increasing temperature. The alignment of the magnetic domains along the external field at high fields would thus vary with magnetic fields and temperature, being less pronounced at low temperatures.

The YCo<sub>3</sub> NPD pattern for 50 K has been refined, assuming a space group  $R-3m$  and a magnetic space group  $*R-3m'$ . The refinement, starting from the ferromagnetic structure with an average MM of  $0.60\mu_B$ , as determined from the vibrating sample magnetometer (VSM) measurements,<sup>3</sup> automatically converged to a ferrimagnetic structure, with Co<sub>2</sub> having an antiparallel MM. The magnetic unit cell is the same as the nuclear unit cell, as there were no extra peaks in the observed patterns. The refinements of the diffraction patterns with (a) crystal structure only and (b) crystal and ferrimagnetic structures are shown in Fig. 2 and the corresponding magnetic moments of the Co atoms and the goodness-of-fit criteria are given in Table II. The  $\chi^2$  values for the refinements of (a) the crystal structure only and (b) the crystal plus ferrimagnetic structures are 16.08 and 14.29, respectively. In the inset plots in Figs. 2(a) and 2(b), the difference between the fits to the (101) peak ( $d=4.2649$  Å) with and without magnetic structure is shown. The fitting with magnetic diffraction included is clearly much better than that for the crystal structure alone. The effect is most noticeable for this reflection because the magnetic diffraction is stronger at larger  $d$  spacings due to the form factor. Thus the experimental data strongly supports the conclusion that, at 50 K, the ground magnetic state for the YCo<sub>3</sub> crystal is ferrimagnetic in nature, with Co<sub>2</sub> atoms having antiparallel spin.

### III. THEORETICAL RESULTS

#### A. Computational details

In our theoretical calculations, we have used the highly accurate full-potential augmented plane-wave + local orbital (FPAPW+lo) method in a scalar relativistic form, as imple-

TABLE II. YCo<sub>3</sub> magnetic moments from neutron powder diffraction for ferrimagnetic structure, refined using GSAS.

		Crystal + ferrimagnetic structures				Crystal structure only
		Starting from VSM average Mz values	Starting from calculated ferro-Mz values	Starting from calculated ferri-Mz values	Using calculated ferri-Mz values	
Results from GSAS refinements						
$\chi^2$		14.27	14.29	14.28	14.35	16.08
$wRp$ (-background)		0.0201	0.0200	0.0200	0.0207	0.0216
$Rp$ (-background)		0.0197	0.0192	0.0194	0.0206	0.0215
Mz ( $\mu_B$ )	Co <sub>1</sub>	0.953(73)	0.880(75)	0.918(74)	1.343	0
	Co <sub>2</sub>	-0.054(51)	-0.108(52)	-0.074(52)	-0.335	0
	Co <sub>3</sub>	0.834(30)	0.792(31)	0.811(30)	0.929	0
	Average	0.650(39)	0.602(41)	0.626(40)		0

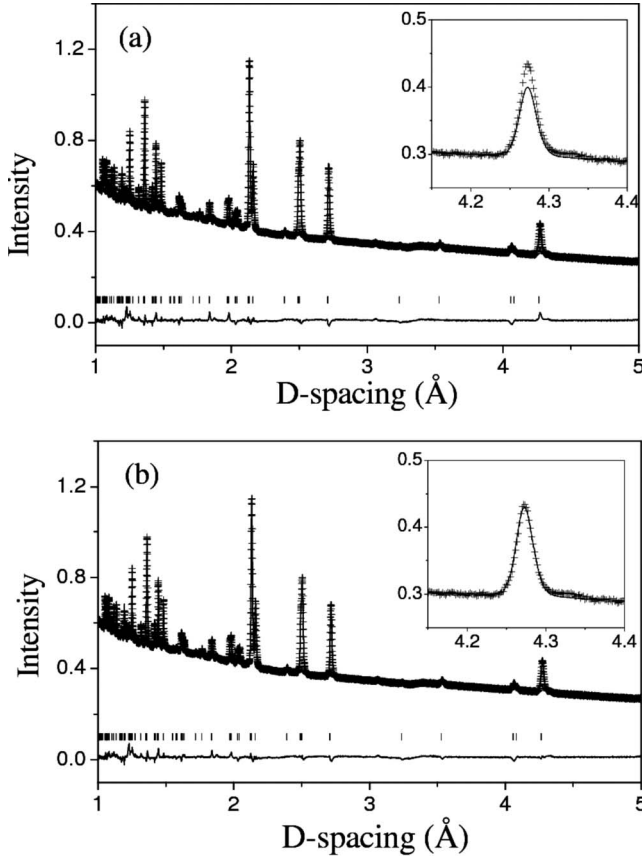


FIG. 2.  $\text{YCo}_3$  NPD refinement: (a) crystal structure only and (b) crystal and ferrimagnetic structure.

mented in the WIEN2k code.<sup>18</sup> These calculations are based on density functional theory (DFT)<sup>19</sup> using the generalized gradient approximation<sup>20</sup> to describe the exchange-correlation functional. The charge density and potential are expanded in spherical harmonics within nonoverlapping atomic spheres and in plane waves in the remaining interstitial regions of the unit cell. Muffin-tin radii  $R_{\text{mt}}$ , of 2.5 a.u. for Y and 2.3 a.u. for Co atoms are used. The wave functions in the interstitial region are expanded in plane waves with a cutoff of  $K_{\text{max}}=8/R_{\text{mt}}$ . The charge density is Fourier expanded up to  $G_{\text{max}}=17$  a.u. The initial basis set includes  $5s$ ,  $5p$ , and  $4d$  valence and  $4s$  and  $4p$  for semicore wave functions for Y, and  $4s$ ,  $4p$ , and  $3d$  valence and  $3s$  and  $3p$  semicore functions at the Co site. These basis functions were supplemented with local orbitals,<sup>21</sup> for additional flexibility in the representation of the semicore states and for reduction of the linearization errors. The accurate tetrahedron integration method was used on a grid of 1000 special  $\mathbf{k}$  points in the whole Brillouin zone (BZ), corresponding to 110  $\mathbf{k}$  points in the irreducible wedge of the BZ.

For  $\text{YCo}_3$ , if one considers only the MM of the Co atoms, there are three possible ferrimagnetic arrangements involving the antiparallel Co atoms, namely, ferri- $\text{Co}_1$  (equivalent to ferri- $\text{Co}_2$ +ferri- $\text{Co}_3$ ), ferri- $\text{Co}_2$ , and ferri- $\text{Co}_3$ . We find that for both ferri- $\text{Co}_1$  and ferri- $\text{Co}_3$ , the self-consistent iterations lead from an initial ferrimagnetic configuration to a ferromagnetic state. However, starting from ferri- $\text{Co}_2$ , self-consistent iteration does stabilize this ferrimagnetic state.

TABLE III. Calculated relative total energies for the nonmagnetic, ferromagnetic, and ferrimagnetic structures with and without spin-orbit coupling (units in meV/primitive cell).

	Without S-O coupling	Including S-O coupling
Ferromagnetic	326.3	5.5
Ferrimagnetic	338.6	0
Nonmagnetic	897.6	435.2

Hence, in the rest of this paper, the ferrimagnetic phase refers specifically to the ferri- $\text{Co}_2$  solution, with  $\text{Co}_2$  atoms having the antiparallel moments.

We use the primitive cell, formulated as  $\text{Y}_3\text{Co}_9$  as our calculation model. The spin-orbit coupling is treated using the second variational approach, as described in Ref. 22. For the calculations performed including spin-orbit coupling, we assume that both the magnetization and the field are parallel to the  $c$  axis, based on the fact that the easy direction of magnetization is along the  $c$  axis.<sup>17</sup> The inclusion of spin-orbit coupling decreases the symmetry. For  $\text{YCo}_3$ , the number of symmetry operations drops from 12 to 4.

### B. Geometric optimization of the simulated lattice

Since the magnetic moments of transition metals generally depend on which sites are occupied and are sensitive to the unit cell volume, much effort has been paid to the full geometrical relaxation of the crystal structure. Geometrical data from our recent synchrotron x-ray refinement given in Table I was used to define the initial structure before relaxation. Firstly, we relaxed the atomic positions globally using the force-minimization technique, by keeping both  $c/a$  and the cell volume ( $V_0$ ) fixed to the synchrotron x-ray experimental values. Then the theoretical equilibrium volume was determined by fixing the optimized atomic positions and the experimental  $c/a$  ratio, and varying the cell volume around  $V_0$ . Finally, the optimized  $c/a$  ratio is obtained by varying  $c/a$ , while keeping the theoretical equilibrium volume fixed at the previously optimal volume. Full geometric relaxation was performed for the ferromagnetic phase without including the spin-orbit coupling. Further relaxation in all other magnetic structures proved unnecessary as the magnitude of the forces (with and without spin-orbit coupling) remained below the convergence criteria ( $0.08 \text{ eV}/\text{\AA}$ ). The parameters obtained from the calculations following geometric relaxation are summarized in Table I, in comparison with the synchrotron x-ray experimental values. We would attribute the small discrepancies to the presence of impurity phases in the experimental sample and to the approximate treatment of exchange correlation in the calculations.

### C. Energetics and the magnetic structure

We have studied the nonmagnetic, the ferromagnetic, and the ferrimagnetic phases both with and without spin-orbit coupling. The total energy values and the magnetization data are summarized in Tables III and IV, respectively. From Table III, one can draw some important conclusions: Firstly,

TABLE IV. Calculated local and averaged magnetic moments (MM) for YCo<sub>3</sub>, with and without spin-orbit (S-O) coupling, and compared with the data from neutron power diffraction experiment.

		Theoretical results					Neutron diffraction experimental results			
		Without S-O coupling			Including S-O coupling					
	Atom	MM ( $\mu_B$ )	Average $\mu_B/\text{Co}$	Atom	MM ( $\mu_B$ )	Average $\mu_B/\text{Co}$	Atom	MM ( $\mu_B$ )	Average $\mu_B/\text{Co}$	
Ferro-	Y <sub>1</sub>	-0.137	1.17	Y <sub>1</sub>	-0.142	1.16				
	Y <sub>2</sub>	-0.172		Y <sub>2</sub>	-0.173					
	Co <sub>1</sub>	1.263		Co <sub>1</sub>	1.251		Co <sub>1</sub>	0.50		
	Co <sub>2</sub>	1.507		Co <sub>2</sub>	1.502		Co <sub>2</sub>	0.35		
	Co <sub>3</sub>	1.329		Co <sub>3</sub>	1.325		Co <sub>3</sub>	0.725		
	Interstitial	-1.278		Interstitial	-1.289					
Ferri-	Y <sub>1</sub>	-0.072	0.62	Y <sub>1</sub>	-0.081	0.61			0.58	
	Y <sub>2</sub>	-0.113		Y <sub>2</sub>	-0.115					
	Co <sub>1</sub>	1.344		Co <sub>1</sub>	1.343		Co <sub>1</sub>	0.70		
	Co <sub>2</sub>	-0.342		Co <sub>2</sub>	-0.335		Co <sub>2</sub>	-0.20		
	Co <sub>3</sub>	0.936		Co <sub>3</sub>	0.929		Co <sub>3</sub>	0.82		
	Interstitial	-0.534		Interstitial	-0.548					

YCo<sub>3</sub> is a strongly magnetic system, as the nonmagnetic state is much higher in energy than either the ferromagnetic or the ferrimagnetic state. Secondly, the ferromagnetic and ferrimagnetic magnetic phases are very comparable in energy. Spin-orbit coupling is found to be important in predicting the “correct” magnetic ground state. In fact, without spin-orbit coupling, the ferromagnetic state is more energetically favorable by 12.3 meV/primitive cell, while when it is included the ferrimagnetic state is more stable by 5.5 meV/primitive cell.

From Table IV, we see that the calculated magnetic moments are not significantly sensitive to the inclusion of spin-orbit coupling. The calculated ferrimagnetic structure has an average MM of  $0.61\mu_B/\text{Co}$ , which is in good agreement with the experimental value for the magnetization ( $0.5\text{--}0.7\mu_B/\text{Co}$ ). For the ferromagnetic state, this value is  $1.16\mu_B/\text{Co}$ , which is in agreement with the calculated ferromagnetic value of  $1.05\mu_B/\text{Co}$  in Ref. 10, but disagrees with the value of  $0.64\mu_B/\text{Co}$  in Ref. 11 and with our own experimental data.<sup>3</sup> According to our calculations, YCo<sub>3</sub> is ferrimagnetic due to the antiparallel alignment of the local moment of the Co<sub>2</sub> atom. For this case, the calculated magnetic moments of the three different Co sublattices (with S-O coupling) are  $1.343\mu_B$  (Co<sub>1</sub>),  $-0.335\mu_B$  (Co<sub>2</sub>), and  $0.929\mu_B$  (Co<sub>3</sub>). Reasonable agreement is thus only achieved between calculation and experiment for the ferrimagnetic structure, particularly for the average MM—considering the fact that the MM in the interstitial region is difficult to assign to any atom and the values of atomic MM refer to within the muffin-tin spheres.

#### D. Field-induced magnetic transitions: a FSM study

##### 1. Ferromagnetic state

In order to elucidate the mechanism of the field-induced magnetic transitions,<sup>12</sup> we have performed a series of FSM

calculations for total MM ranging from 0 to  $16\mu_B$ . The total MM is given by the difference in the number of spin-up and spin-down electrons in the primitive cell. For each fixed value of the MM, a self-consistent converged solution is obtained. For the ferromagnetic phases, the total energy and the corresponding changes of local MM on the individual Co sites are given as a function of the total MM in Fig. 3. In this case, the FSM study identified only one minimum in the total

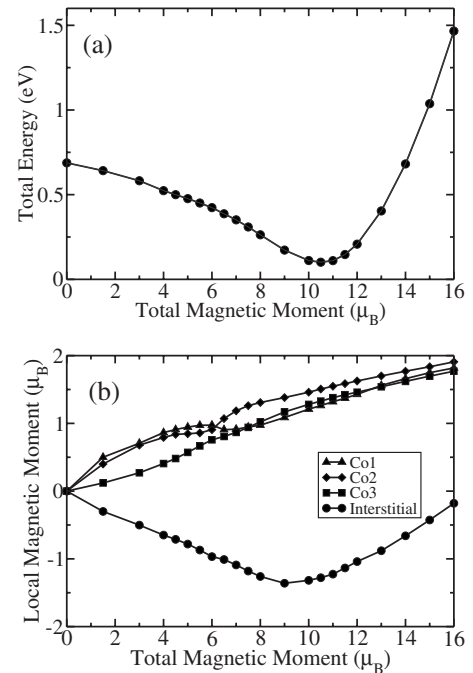


FIG. 3. FSM calculations on the ferromagnetic states. (a) Total energy versus total magnetic moment (MM); (b) three different Co atoms local MM versus total MM.

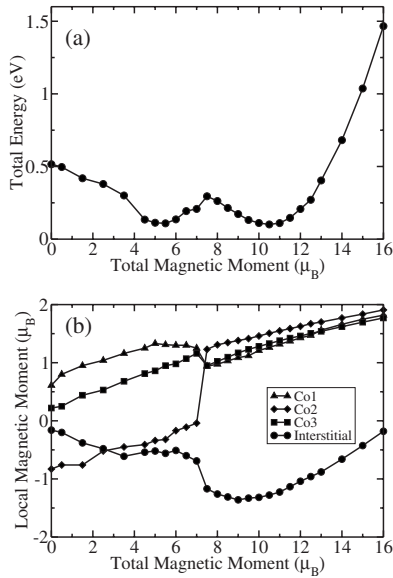


FIG. 4. FSM calculations for the  $\text{YCo}_3$  ferrimagnetic state. (a) Total energy versus total magnetic moment (MM); (b) three different Co atoms MM versus total MM. In (a),  $0 < \text{total MM} < 6\mu_B$ , the structure is ferrimagnetic, with a total MM between 6 and  $7\mu_B$ ,  $\text{Co}_2$  is nearly nonmagnetic. For a total  $\text{MM} > 7.5\mu_B$ , the structure is ferromagnetic.

energy versus MM curve, which is located around  $10.5\mu_B$  ( $1.16\mu_B/\text{Co}$ ) and consistent with our normal spin-polarized calculation. At this point, the Fermi energy  $E_F(\text{up}) = E_F(\text{down})$ . If we follow the energy curve to higher values of the MM, we observe a sharp increase in the energy. If the average moment on the Co sites was  $0.6\mu_B/\text{Co}$  as derived from the NPD data and as calculated in Ref. 11, the total MM would be around  $5.4\mu_B$ . However, there is no indication of a local minimum in the energy curve at this value of the total moment. Hence we can state clearly that in our calculation there is no reason to believe that  $\text{YCo}_3$  has a ferromagnetic structure with an average moment  $0.5\text{--}0.7\mu_B/\text{Co}$ . As for the local MM of the three Co atoms, there is a clear change around a total  $\text{MM} = 6\text{--}7\mu_B$ , where the MM of  $\text{Co}_1$  decreases and  $\text{Co}_2$  increases dramatically. After this region, all three local moments increase gradually but the  $\text{Co}_2$  atom now has a larger MM than  $\text{Co}_1$  and  $\text{Co}_3$ .

## 2. Ferrimagnetic state

A similar FSM approach has been applied for the ferrimagnetic (ferri- $\text{Co}_2$ ) phase. The calculated total energy and the MM of the three Co sites as a function of the total MM are presented in Fig. 4. We note that it is only for low values of the total MM, ranging from  $\text{MM} = 0$  to  $7\mu_B$ , that the self-consistent solution converges to a ferrimagnetic solution. For  $\text{MM} > 7.5\mu_B$ , the initial ferrimagnetic configuration will automatically converge to a ferromagnetic solution. Two distinct minima are observed in the total energy versus total MM curve. One is in the ferrimagnetic region, located at  $\text{MM} = 5.5\mu_B$ , the other is in the ferromagnetic region, located at  $\text{MM} = 10.5\mu_B$ , the latter being the same as found in the ferromagnetic studies. Furthermore, the ferrimagnetic solu-

tion, corresponding to  $0.61\mu_B/\text{Co}$ , is consistent with the experimental value ( $0.5\text{--}0.7\mu_B/\text{Co}$ ) and our direct spin-polarized calculation for ferrimagnetic phase. We therefore propose that this is the starting point in the magnetic transition process, and that the minimum for the ferromagnetic solution, corresponding to  $1.16\mu_B/\text{Co}$ , is consistent with the terminal point ( $1.23\mu_B/\text{Co}$ ) in the magnetic transition. We believe this is the fully saturated MM. We also observed a small flat step around  $\text{MM} = 6.5\mu_B$ , which can be attributed to the first magnetic transition found in the experiment. Around this point, the  $\text{Co}_2$  atom is nearly nonmagnetic. Based on the FSM results, we predict that the magnetic transition is a process by which the  $\text{YCo}_3$  crystal changes from the ferrimagnetic ground state and terminates as a ferromagnet under external high magnetic field. The origin of the magnetic transition is now clear: the ferrimagnetic  $\text{Co}_2$  atoms first lose their MM becoming nonmagnetic and then change to a ferromagnetic alignment under the influence of a high magnetic field [see Fig. 3(b)]. This can be understood as a field-induced spin-flip process under high external magnetic field.

In summary, based on first-principles DFT-FSM calculations, the two successive magnetic transitions observed under ultrahigh magnetic field can be described as follows: If one only considers the spin on  $\text{Co}_2$  atoms, the ferrimagnetic phase first undergoes a transition by losing the antiparallel alignment of the  $\text{Co}_2$  local moment. This is followed by the  $\text{Co}_2$  atom becoming rapidly ferromagnetic and terminating at the saturated moment. During this process, the local magnetic moments of  $\text{Co}_1$  and  $\text{Co}_3$  first increase gradually until the first transition after which they decrease. After the  $\text{Co}_2$  changes to the ferromagnetic alignment, the three different Co atoms gradually accumulate further local moments with further increase in the applied field.

## E. Electronic structure: DOS analysis

From the above analysis, both ferrimagnetic and ferromagnetic states of  $\text{YCo}_3$  can coexist due to their very competitive total energies. Furthermore, while the ferrimagnetic phase is predicted to be the ground state, the ferromagnetic phase can be obtained under high magnetic field. Details of the electronic structure are helpful in understanding and interpreting this interesting behavior. To this end, we have calculated the DOS and atomic local DOS (LDOS) for the ferrimagnetic and ferromagnetic phases of  $\text{YCo}_3$ , as displayed in Figs. 5 and 6, respectively.

By careful analysis of these DOS, one can draw important conclusions: Both the  $\text{Y}_1$  and the  $\text{Y}_2$  atoms contribute mainly to the DOS in the region above the Fermi energy ( $E_F$ ), while the LDOS of Co sites are located near to or below  $E_F$ , indicating that there is charge transfer from the Y atoms to the Co atoms. Generally, for both Y atoms and Co atoms, broad  $s$  and  $p$  bands are observed in addition to the localized  $d$  bands. The magnetic properties for the ferrimagnetic and ferromagnetic states are mainly determined by the  $d$  band of the Co atoms. Not surprisingly, the most distinctive difference between the DOS and LDOS for the ferrimagnetic and ferromagnetic phases lies in the LDOS of  $\text{Co}_2$ . The other LDOS plots are rather similar in the two structures. This also indi-

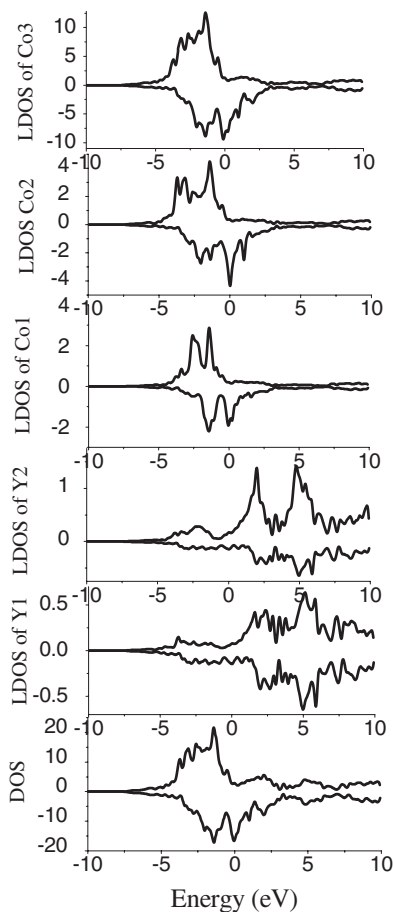


FIG. 5. Total DOS (a) and local DOS [(b)–(f) in the order of Y<sub>1</sub>, Y<sub>2</sub>, Co<sub>1</sub>, Co<sub>2</sub>, and Co<sub>3</sub>, respectively] of the ferromagnetic state of YCo<sub>3</sub>.

cates that the rigid band model can be applied as a first approximation to the analysis of the DOS, particularly for the ferromagnetic structure. For this structure, the LDOS of the three Co sites around the  $E_F$  are quite similar. This finding can explain the similar behavior of the magnetic moments of the three Co atoms under increasing magnetic field at high fields [see the range  $MM > 10.5\mu_B$  in Fig. 4(b)]. Also we can see that the total DOS of the ferrimagnetic structure is very oscillatory, showing complex peaks around  $E_F$ . This is helpful in understanding the magnetic transitions. In a simple rigid band picture, we may focus on the ferrimagnetic Co<sub>2</sub>. The Fermi energy ( $E_F$ ) is located at the right-hand side of the highest DOS peak, so a small upward shift due to the magnetic field can result in significant magnetic property changes. The first transition can be understood as being due to the  $E_F$  moving to the DOS valley where the total energy will reach a local minimum. A further right shift of the  $E_F$  leads to higher energies and when  $E_F$  climbs over the next DOS peak, the system will change into a ferromagnetic state. However, the DOS near  $E_F$  is too complex to provide a clear interpretation of the field-induced transition using the simple rigid band model. Changes in the general shape of the DOS indicate that complicated field effects are important for a quantitative understanding.

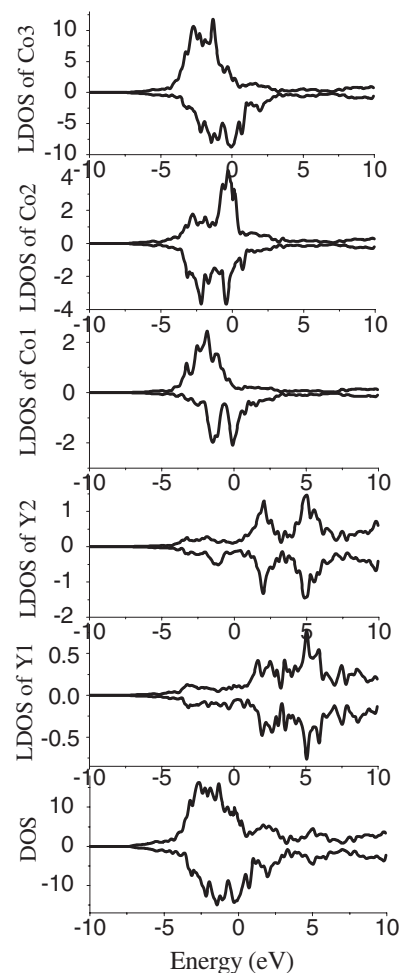


FIG. 6. Total DOS (a) and local DOS [(b)–(f) in the order of Y<sub>1</sub>, Y<sub>2</sub>, Co<sub>1</sub>, Co<sub>2</sub>, and Co<sub>3</sub>, respectively] of the ferrimagnetic state of YCo<sub>3</sub>.

#### IV. FURTHER DISCUSSION

Since the theoretical values of the magnetic moments are somewhat different from the values obtained from the NPD analysis, the calculated values obtained for the ferrimagnetic structure were put into GSAS and kept fixed to see whether they were consistent with the NPD data. The  $\chi^2$  value is 14.35, which is not quite as good as the best fit, but obviously better than the fit for the crystal structure only. The values of the magnetic moments were then allowed to refine from this starting point, resulting in the  $\chi^2$  value decreasing to 14.28, and the values of the resultant magnetic moments turn out to be very close to those of the best previous fit. From this, we conclude that there is a significant difference between the experimental and theoretical moments. The results of these refinements are also listed in Table II.

NPD is the primary technique used for determining magnetic structures. Polarized neutron scattering and the use of a single crystal sample can increase the sensitivity to details of the structure. However, sometimes diffraction alone is still not sufficient to determine a unique solution without ambiguity. YCo<sub>3</sub> presents a particular challenge to the neutron diffraction approach due to two intrinsic factors. The first is

that the Y nuclei have a much larger coherent cross section than the Co nuclei [Y:  $7.55 \times 10^{-28} \text{ m}^2$  and Co:  $0.779 \times 10^{-28} \text{ m}^2$  (Ref. 23)]. Thus, in the neutron diffraction spectra of the nonmagnetic phase, a nonmagnetic Y atom makes a much more significant contribution to the diffraction pattern than a magnetic Co atom. Secondly, the MM of Co atoms in  $\text{YCo}_3$  ( $\sim 0.60 \mu_B/\text{Co}$ ) is quite small, much less than, for example, the  $1.7 \mu_B/\text{Co}$  found in pure Co. Thus, one would expect that the neutron powder diffraction pattern is dominated by the nuclear diffraction from the crystal structure and is only slightly influenced by the magnetic diffraction, even for a single crystal sample. Another difficulty associated with the experimental determination stems from the sample preparation. The Y-Co phase diagram is very complicated and a sample of nominal composition  $\text{YCo}_3$  usually contains impurity phases such as  $\text{YCo}_5$ ,  $\text{YCo}_2$ ,  $\text{Y}_2\text{Co}_7$ , and  $\text{Y}_2\text{Co}_{17}$ , which exhibit diverse magnetic properties. These will clearly tend to increase the optimum  $\chi^2$  value.

The magnetic properties of  $\text{YCo}_3$  also present a challenge to theoretical simulation. Although we have predicted the correct magnetic ground state by including the spin-orbit coupling effect, the ferrimagnetic and ferromagnetic phases are very comparable in total energy. We assume that a more exacting treatment of exchange and correlation effect would improve the results.

We also note that some compounds with the same crystal structure, for example,  $\text{DyCo}_3$ , and  $\text{ErCo}_3$ , are also ferrimagnetic,<sup>8,25,26</sup> but here the ferrimagnetism is due to the  $f$  electrons of the heavy metal element (Dy, Er), not the Co atoms. In  $\text{YCo}_3$ , although the Y atoms are magnetic, the moments are very small, say  $\sim 0.1 \mu_B/\text{Y}$  (see Table IV) and are due to conduction electron polarization. Thus, the ferrimagnetism in  $\text{YCo}_3$  is fundamentally different in nature from these compounds. To demonstrate this, we have also performed calculations for the  $\text{Y}_2\text{Co}_7$  system, which has same space group and a similar structure as  $\text{YCo}_3$ . Our results here are in excellent agreement with Lemaire's experiment<sup>7</sup> and other calculations,<sup>11,12</sup> which all suggest that it is indeed ferromagnetic—but there are still small negative magnetic moments associated with the Y atoms. Magnetic transitions due to the change in the magnetic moments on the Co atoms are also observed in the stoichiometric ferromagnetic compound,  $\text{ThCo}_5$ .<sup>24</sup> Here, under zero magnetic field, the Co moment on the 3g site ( $0.9 \mu_B$ ) is lower than that of the 2c site ( $1.2 \mu_B$ ) but, in a high magnetic field, equal moments ( $1.5 \mu_B$ ) are observed. However, this behavior also differs in nature from the magnetic transition in  $\text{YCo}_3$ .

Conceptually, for a given system containing various non-equivalent magnetic atoms, it is necessary to consider all the possible magnetic structures involved to determine the ground state. Based on this, then one can hope to understand the magnetic phase transition exhibited under external mag-

netic field. In the present study, we investigate the ferromagnetic and ferrimagnetic phases of  $\text{YCo}_3$  on an equal footing by employing both first-principles calculations and neutron diffraction experiments and establish that the new ferrimagnetic phase is actually the ground state and explain the phase transitions. Similar motivation has been demonstrated in the transition metal doped dilute magnetic semiconductors.<sup>25,26</sup>

## V. SUMMARY

In summary, the magnetic properties of  $\text{YCo}_3$  present an interesting and challenging topic. By combining neutron powder diffraction and first-principles DFT calculations, we have examined the magnetic ground state, the magnetic structure, and the magnetic transitions under ultrahigh magnetic fields and the temperature-dependent magnetization. Both the ferromagnetic and ferrimagnetic phases are examined on an equal footing. Several important conclusions can be drawn from the results obtained:

(1) Both ferromagnetic ( $1.16 \mu_B/\text{Co}$ ) and ferrimagnetic (ferri- $\text{Co}_2$ ,  $0.61 \mu_B/\text{Co}$ ) phases have been characterized by numerical fitting of the NPD data taken at 50 K and studied by first-principles DFT calculations. The NPD data refines unambiguously to the ferrimagnetic state. However, in the *ab initio* calculations, the two phases are very comparable in their fully relaxed energy. Indeed, it is necessary to introduce spin-orbit coupling to predict the correct magnetic ground state. Our studies thus suggest that  $\text{YCo}_3$  is ferrimagnetic in nature at 50 K with the  $\text{Co}_2$  atoms having antiparallel moments, rather than the previously widely believed ferromagnetic arrangement. This conclusion is also consistent with the variation of the magnetization with temperature and applied field.

(2) Interestingly, for  $\text{YCo}_3$ , both the ferrimagnetic state and the ferromagnetic state are physically achievable. The fixed spin moment technique allows us to understand the two successive field-induced magnetic transitions observed under ultrahigh external magnetic field. The magnetic transitions are believed to start from the ferrimagnetic state ( $0.61 \mu_B/\text{Co}$ ) at low temperatures and  $\text{Co}_2$  atoms change from antiparallel to nonmagnetic for the first transition and then to ferromagnetic during the second transition and terminate in this state ( $1.16 \mu_B/\text{Co}$ ). This observation confirms that the changes in magnetization under high fields are mainly due to a spin-flip process on the  $\text{Co}_2$  atom.

## ACKNOWLEDGMENTS

We want to thank M. Yamaguchi at Yokohama National University, Japan for helpful discussions. All calculations in this study were performed on facilities in the Centre for High Performance Computing at the University of Salford funded by the HEFCE and IBM (U.K.) through the JREI scheme.

- \*Author to whom correspondence should be addressed; i.morrison@salford.ac.uk
- <sup>1</sup>M. Yamaguchi, H. Ikeda, T. Ohta, T. Goto, and T. Katayama, *Solid State Commun.* **53**, 383 (1985).
  - <sup>2</sup>M. I. Bartashevich, H. A. Katori, T. Goto, I. Yamamoto, and Y. Yamaguchi, *Physica B* **210**, 135 (1994).
  - <sup>3</sup>J. Liu, D. P. Broom, P. A. L. Georgiev, and D. K. Ross, *J. Alloys Compd.* **356-357**, 174 (2003).
  - <sup>4</sup>X. Y. Cui, J. Liu, I. Morrison, and D. K. Ross, *J. Alloys Compd.* **404-406**, 136 (2005).
  - <sup>5</sup>J. N. Huiberts, R. Griessen, J. H. Rector, R. J. Wijngaarden, J. P. Dekker, D. G. de Groot, and N. J. Koeman, *Nature (London)* **380**, 231 (1996).
  - <sup>6</sup>J. Liu, X. Y. Cui, P. A. Georgiev, I. Morrison, D. K. Ross, M. A. Roberts, K. A. Andersen, M. Telling, and D. Fort, *Phys. Rev. B* **76**, 184444 (2007).
  - <sup>7</sup>R. Lemaire, *Cobalt (Engl. Ed.)* **33**, 201 (1966).
  - <sup>8</sup>E. Kren, J. Schweizer, and F. Tasset, *Phys. Rev.* **186**, 479 (1969).
  - <sup>9</sup>J. Inoue and M. Shimizu, *J. Phys. F: Met. Phys.* **15**, 1511 (1985).
  - <sup>10</sup>R. Coehoorn, *J. Magn. Magn. Mater.* **99**, 55 (1991).
  - <sup>11</sup>M. Yamaguchi and S. Asano, *J. Magn. Magn. Mater.* **168**, 161 (1997).
  - <sup>12</sup>M. I. Bartashevich, T. Goto, M. Yamaguchi, and I. Yamamoto, *Physica B* **294-295**, 186 (2001).
  - <sup>13</sup>V. L. Moruzzi, A. R. Williams, A. P. Malozemoff, and R. J. Gambino, *Phys. Rev. B* **28**, 5511 (1983).
  - <sup>14</sup>K. Schwartz and P. Mohn, *J. Phys. F: Met. Phys.* **14**, L129 (1984).
  - <sup>15</sup>For examples, H. J. F. Jansen, *J. Appl. Phys.* **81**, 3866 (1997); H. Yamada, K. Terao, H. Ohta, T. Arioka, and E. Kulatov, *J. Phys.: Condens. Matter* **11**, L309 (1999); S. L. Qiu, *Phys. Rev. B* **60**, 56 (1999); J. H. Lee, Y. C. Hsue, and A. J. Freeman, *ibid.* **73**, 172405 (2006); X. Y. Cui, B. Delley, A. J. Freeman, and C. Stampfl, *Phys. Rev. Lett.* **97**, 016402 (2006).
  - <sup>16</sup>A. C. Larson and R. B. Von Dreele, Los Alamos National Laboratory Report No. LAUR 86-748, 1994 (unpublished).
  - <sup>17</sup>M. I. Bartashevich, T. Goto, M. Yamaguchi, I. Yamamoto, and A. V. Andreev, *Solid State Commun.* **82**, 201 (1992).
  - <sup>18</sup>P. Blaha, K. Schwarz, G. K. H. Madsen, D. Kvasnicka, and J. Luitz, WIEN2k, (Vienna University of Technology, An Augmented Plane Wave + Local Orbitals Program for Calculating Crystal Properties, revised edition 2001).
  - <sup>19</sup>P. Hohenberg and W. Kohn, *Phys. Rev.* **136**, B864 (1964); W. Kohn and L. J. Sham, *Phys. Rev.* **140**, A1133 (1965).
  - <sup>20</sup>J. P. Perdew, K. Burke, and M. Ernzerhof, *Phys. Rev. Lett.* **77**, 3865 (1996).
  - <sup>21</sup>D. Singh, *Phys. Rev. B* **43**, 6388 (1991).
  - <sup>22</sup>J. Kunes, P. Novak, M. Divis, and P. M. Oppeneer, *Phys. Rev. B* **63**, 205111 (2001).
  - <sup>23</sup>V. F. Sears, *Neutron News* **3** (3), 26 (1992).
  - <sup>24</sup>D. Givord, J. Laforest, and R. Lemaire, *Physica B & C* **86-88**, 204 (1977).
  - <sup>25</sup>X. Y. Cui, J. E. Medvedeva, B. Delley, A. J. Freeman, N. Newman, and C. Stampfl, *Phys. Rev. Lett.* **95**, 256404 (2005).
  - <sup>26</sup>X. Y. Cui, J. E. Medvedeva, B. Delley, A. J. Freeman, and C. Stampfl, *Phys. Rev. B* **75**, 155205 (2007).